Contribution to System Frequency Stability and Resilience from PV Plants: A Closed-loop System Identification Approach

Mehdi Ghazavi Dozein
School of Electrical and Electronic Engineering
The University of Melbourne
Melbourne, Australia
mghazavi@student.unimelb.edu.au

Gilles Chaspierre
Department of Electrical Engineering and Computer Scinece
University of Liège
Liège, Belgium
g.chaspierre@ulg.ac.be

Pierluigi Mancarella
School of Electrical and Electronic Engineering
The University of Melbourne
Melbourne, Australia
pierluigi.mancarella@unimelb.edu.au

***Abstract*— The rapid uptake of renewable energy resources and displacement of synchronous generators may pose threats to system frequency stability and resilience. Starting from the August 2018 separation event in Australia, this work models and discusses how utility-scale PV plants could contribute to frequency stability and resilience of islanded areas following separation events. In this regard, a converter-based dynamic equivalent of aggregated PV power plants is proposed which takes into account possible practical issues such as measurement and coordination delays. The unknown parameters of the proposed model are identified through a novel closed-loop identification process based on least-square minimization. Also, a simplified model is constructed to reproduce the system frequency during the event under study, thereby capturing continuous impact of PV response on the frequency. The proposed aggregated model can considerably reduce the complexity of frequency stability analysis as well as its processing time while capturing with good fidelity the frequency response from PV farms.**

Keywords*— Dynamic equivalent model, Frequency stability, Identification methods, Separation events, System resilience, Utility-scale PV plants*.

I. INTRODUCTION

Power systems are evolving towards massive penetration of renewable energy resources, including utility-scale and distributed photovoltaic (PV) plants, to leverage their economic and environmental advantages [1]. Regarding the operation of PV-rich power systems, one of the main issues is related to frequency instability which corresponds to generation-load mismatch and may lead to cascading failures in the form of generation trip, load shedding, or even splitting of the system into islanded areas [2]. Technically, a system with adequate frequency control ancillary services (FCAS) is more likely to regain a stable equilibrium point following frequency contingencies [2]. However, the increase of PV penetration and the subsequent decline in synchronous generation drives power systems into low-inertia conditions which may result in higher rate of change of frequency (RoCoF) values following disturbances, also meaning faster frequency dynamics in general. It is therefore necessary to model the system adequately to be able to capture such fast frequency behaviour. For short-term frequency stability analysis, electromagnetic transient (EMT) models or transient stability models have been mostly employed, which comprise numerous differential-algebraic equations (DAEs) to provide proper representation of power system components [3]. Moreover, there are practical evidence that transmission-connected PV units are required by grid-codes to participate in primary frequency response while the frequency is beyond the normal frequency operating band [4], [5]. Hence, it is also crucial to employ an accurate dynamic model for PV power plants to avoid missing their impact on system frequency characteristics, especially when PV penetration level and subsequently their frequency response may be substantial. However, considering a detailed PV dynamic model along with its associated energy conversion systems for a large number of transmission-connected PV units significantly increase the difficulty in frequency dynamics studies because of the high degree of complexity and order of the system model, which can result in excessive computational time. Consequently, there is a need to come up with suitable dynamic models of PV units for frequency stability and resilience analysis which could effectively reduce the complexity of dynamic modelling without compromising the PV frequency response as seen by the external grid.

Several solutions have been proposed to cope with the complexity of system dynamics studies imposed by equipment dynamic models, such as frequency-dependent network equivalents [6], dynamic phasors [7], modal methods [8], coherency methods [9], and measurement-based (simulation-based) methods [3]. With regards to conventional large-scale transmission networks, previous works have mainly increased the computation efficiency through simplification of synchronous generator model [10] or developing a dynamic equivalent model for a group of synchronous machines through coherency-based methods [11]. Regarding renewable-rich power systems, previous works have mainly worked on developing suitable dynamic equivalent models for active distribution networks to assess their impact on system frequency dynamics [12]. Indeed, previous studies on combined transmission-distribution system dynamics have mainly tried to deal with complexity emerging from active distribution networks. Therefore, the complexity coming from dynamic modelling of transmission-connected converter-based technologies, in particular PV farms, has not been well treated in frequency stability analysis thus far. This paper introduces a dynamic equivalent model for aggregated utility-scale PV farms to reduce the complexity of frequency stability analysis corresponding to numerous transmission-connected PV plants. The proposed model is a converter-based dynamic model which retains the physical model of large-scale PV plants in an equivalent form. The parametrization of the equivalent model can be performed through several approaches such as system truncation methods [13], artificial neural network based (ANN-based) methods [14], or measurement-based (simulation-based) identification schemes [3], [15]. Regarding measurement-based identification methods, most previous studies used an open-loop identification approach in which a constant measured frequency is considered as an input signal of the optimization process, thereby ignoring the continuous impact

of the *study zone* on the system dynamic characteristics [3], [12], [15]. In the context of dynamic equivalencing, a *study zone* refers to the parts of the power system for which there is the aim to develop a dynamic equivalent model or lower-order model [3], [16]. As the frequency response from utility-scale PV plants in high PV-rich power systems may have a considerable impact on system frequency behaviour, their dynamic equivalencing with an open-loop identification approach can potentially lead to inaccuracy in both the model and the system frequency dynamics. This may also lead to inaccurate analysis of frequency-dependent mechanisms such as activation of under-frequency load shedding (UFLS), over-frequency generation trip, or emergency protection schemes on interconnectors.

This paper, first, proposes a novel closed-loop identification process based on least-square minimization which considerably improves the accuracy of the dynamic equivalent model in reproducing the system frequency. In fact, the proposed closed-loop identification process employs a simplified system model to reproduce the frequency during the event under study, thereby taking into account the continuous impact of aggregated frequency response from utility-scale PV plants on the system frequency. Second, the proposed approach is developed further to take into account possible practical issues, such as measurement and coordination delays, which might lead to failure in effective frequency support from PV. For the sake of validation, the performance of the proposed dynamic equivalencing approach is evaluated through a comprehensive study on the dynamic behaviour of utility-scale PV plants during the August 2018 separation event in Australia [17]. Finally, it will be discussed how PV power plants contributed to system resilience by reducing the likelihood of over-frequency generation disconnection during the August 2018 event.

The main contributions of the paper are as follows:

- A converter-based dynamic equivalent model for aggregated utility-scale PV plants to reduce the complexity of frequency stability analysis;
- A closed-loop identification process based on least-square optimization to increase the accuracy of the dynamic equivalent model;
- Highlighting the benefits from PV frequency response to system frequency stability and resilience following extreme events in the context of the August 2018 separation event in Australia;
- Validation of the proposed dynamic equivalencing approach through a comprehensive study on the August 2018 event in Australia.

II. The Proposed Aggregated Dynamic Equivalent Model of Utility-Scale PV Plants

The proposed converter-based dynamic equivalent model, shown in Fig. 1, aggregates the impact of frequency responses from large-scale PV plants on system frequency characteristics. This equivalent model is intuitive as it maintains the generic model of two-stage transmission-connected PV units which provides enhanced flexibility in frequency response provision [18-19]. The DC-AC grid-side converter (GSC) accounts for DC-link voltage control as well as output reactive power management while the DC-DC converter is responsible to maintain the operating active power output (P_{PV}) at the desired stable level (P^*). Furthermore, *PI* blocks stand for proportional-integral controllers. For further details, the reader can refer to [19] to understand how control loops can be designed. Each PI controller, including phase-locked loop (PLL), includes two state variables. Further, current and voltage outputs of aggregated PV array (i, u_{PV}) and DC-AC converter (V, I) are other state variables. Therefore, a PV plant model, as shown in Fig. 1, consists at least 14 state variables.

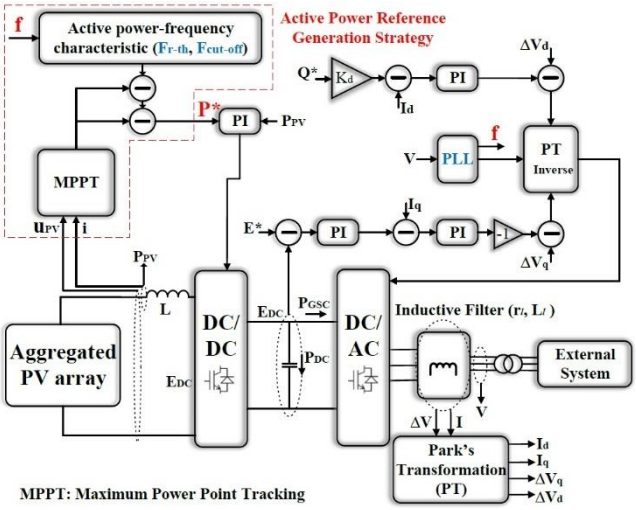

Fig. 1. The proposed dynamic equivalent model of utility-scale PV units including power conversion systems and their associated control loops

As illustrated in Fig. 2, a utility-scale PV plant can normally deliver maximum power (P_{MPP}) while the frequency is within the normal operating band ($f < F_{r-th}$). However, PV farms start to deliver over-frequency droop response to the system once the frequency goes beyond F_{r-th}. The PV unit output will then set to zero if the frequency is above the cut-off frequency ($f \geq F_{cut-off}$), thereby participating with full capacity into over-frequency control [5]. The over-frequency response from PV power plants can potentially contribute to system resilience by maintaining the system frequency outside of the operating region of frequency control emergency schemes such as over-frequency generation shedding (OFGS).

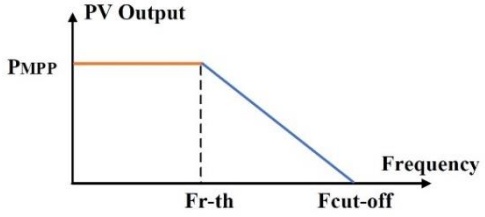

Fig. 2. The typical active power-frequency characteristic for utility-scale PV plants [5]

There are two main common reasons accounting for the different frequency response behaviour that may arise from different utility-scale PV plants. Firstly, grid-code requirements usually parametrize the active power-frequency characteristic for utility-scale PV units. Thus, utility-scale PV units installed in different years might have different frequency settings while grid-codes are updated. Considering the Australian grid-code requirements [4] as an instance, PV units which have been installed prior to 2015 do *not* need to provide over-frequency droop response, differently from those that have been installed after 2016 which, instead, do [4]. Secondly, the frequency deviations seen by utility-scale PVs located at different points of connection may differ from

each other as they are correlated to the disturbance size and location [21]. This can potentially lead to the delay in response provision from PV units *electrically* located far from the fault location [21]. Therefore, the active power-frequency characteristic of the proposed dynamic equivalent model, as well as its overall PLL delay, need to capture the aggregated frequency response from multiple PV power plants. This paper employs a measurement-based system identification method to identify the parameters of active power-frequency characteristic (F_{r-th}, $F_{cut-off}$), as well as the aggregated PLL delay, as detailed later. Furthermore, from a practical point of view, PV plants might not be able to efficiently provide primary frequency response due to potential technical issues such as coordination and measurement delays [17]. Therefore, such practical issues must also be considered in the developed dynamic equivalent models. In this work, an active power reference generation strategy, shown in Fig. 3, is proposed to take into account possible measurement delays as well as coordination delays. As illustrated in Fig. 3, both coordination delay and measurement delay are shown through generic exponential delay function in the Laplace domain with different time delays (r_m, r_c) which will be identified through the proposed identification method.

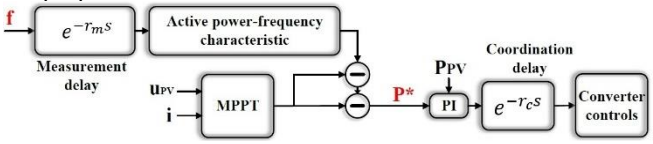

Fig. 3. The proposed active power signal generation strategy which includes measurement delays as well as coordination delays

III. Closed-loop Parameter Identification Process of The Proposed Dynamic Equivalent Model

In this work, a measurement-based system identification approach is put forward to adjust the unknown parameters of the aggregated model in order to minimize the least-square error between the frequency response delivered by the aggregated dynamic model and the actual frequency response provided by utility-scale PV plants during the event under study.

A. Formulation of the Identification Process as an Optimization Problem

Throughout the identification process, the aim is to adjust the unknown parameters in the vector $\boldsymbol{\theta}$ so as to *minimize* the following objective function:

$$\varepsilon_1(\boldsymbol{\theta}) = \frac{1}{N}\sum_{k=0}^{N}\left[P(k) - \hat{P}(k,\boldsymbol{\theta})\right]^2 \quad (1)$$

under the constraints (2):

$$\boldsymbol{\theta}^L \le \boldsymbol{\theta} \le \boldsymbol{\theta}^U \quad (2)$$

Where $\boldsymbol{\theta}^L$ and $\boldsymbol{\theta}^U$ are lower and upper bounds of $\boldsymbol{\theta}$, $P(k)$ is the *actual* discrete time evolution of the total active power delivered by utility-scale units during the event under study, $\hat{P}(k,\boldsymbol{\theta})$ is the *simulated* discrete time evolution of the active power delivered by the aggregated model of PV units, k is the discrete time counter used by the time-domain simulation solver, while the maximum number of discrete time simulation is denoted by N. Further, the $\boldsymbol{\theta}$ vector includes F_{r-th} (the frequency at which the aggregated PV model starts the over-frequency droop response), $F_{cut-off}$ (the frequency at which the output power reaches zero), and PLL delay (δ_{PLL}) (i.e., $\boldsymbol{\theta} = [F_{r-th}, F_{cut-off}, \delta_{PLL}]$). Considering measurement and coordination delays, the $\boldsymbol{\theta}$ vector needs to be expanded further to $[F_{r-th}, F_{cut-off}, \delta_{PLL}, r_m, r_c]$ to include the unknown time delays as well. It is also possible to combine measurement and coordination delays together as the aggregated time delay affects the quality of frequency response from PV units. Thus, one of the technical delays (e.g., r_m) can be set to an arbitrary value while the total delay is combined into another time delay type (e.g., r_c) to speed up the identification process.

It is not possible to derive an analytical expression of $\varepsilon_1(\boldsymbol{\theta})$ as $\hat{P}(k,\boldsymbol{\theta})$ is obtained from time-domain simulation. Therefore, classical optimization techniques [22-23] cannot be used to minimize the objective function in (1). In this work, differential evolution (DE) algorithm [24] is used to solve the least-square constrained minimization problem (1)-(2). The DE algorithm is a population-based method which mainly includes three operators: crossover, mutation, and selection. Also, the performance of DE algorithm is highly dependent to three control parameters: mutation constant (F), crossover constant, and size of population. To improve probability and speed of convergence, *F* is randomly selected in the range of [0.5, 1] while the crossover probability is set to 0.9 [25]. The population size is decided to be 10 times larger than the number of unknown parameters as suggested in [24]. Each generation involves creation of a new population from the current population members $x_{i,g}$ where i indexes the vectors that make up the population and g indexes the generation. In this work, the *local-to-best* strategy has been chosen since it attempts a balance between robustness and fast convergence [25]. This strategy generates mutant vectors $v_{i,g}$ by randomly selecting two members of the population $x_{r1,g}$ and $x_{r2,g}$ as below:

$$v_{i,g} = x_{i,g} + F\left(best_g - x_{i,g}\right) + F\left(x_{r1,g} - x_{r2,g}\right) \quad (3)$$

Where $x_{i,g}$ and $best_g$ are the i th member and the best member, respectively, of the previous population. If the mutant parameter vector $v_{i,g}$ has a better objective function than $x_{i,g}$, then $v_{i,g}$ replaces $x_{i,g}$ in the population. For further study on the DE method, the reader can refer to [24-25].

B. The Proposed Closed-loop Identification Process

Considering a high penetration of utility-scale PV plants in transmission networks, and assuming they are capable and enabled to actively provide frequency response, their aggregated frequency response, and eventually the associated impact on system frequency dynamics, may be substantial. In other words, as far as PV units are responding to frequency excursions by changing their active power output, they are continuously affecting the system frequency dynamics, and this continuous impact may be considerable while transmission network is penetrated with large volume of PV. Therefore, it is necessary to consider the aforesaid continuous impact while running the identification process to increase the accuracy of dynamic equivalencing method. In this work, a closed-loop identification process, illustrated in Fig. 4, is suggested which employs a simplified equivalent test-system to emulate the frequency recorded during the event under study, thereby taking into account the continuous impact of the aggregated response from PV units on the system frequency dynamics. As shown in Fig. 4, in this case the *study zone* corresponds to the part of the system that encounters over-frequency condition, while the rest of the system is modelled by a Thevenin equivalent model along with an equivalent load. The *study zone* includes an equivalent synchronous machine, as well as an equivalent load, which represent the area inertia at the time of the event under study. The frequency of *study zone* is then reproduced using the angular speed of the equivalent synchronous machine. This

simulated frequency is then used by the proposed aggregated dynamic equivalent model to obtain its aggregated active power output during the event under study. The *study zone* also consists of an equivalent impedance (R, X) which represents a simplified equivalent model of transmission lines and transformers in the area under study. Finally, it is also important to correctly model load dependency to system frequency. In this paper, load sensitivity to frequency deviation within the study zone is modelled through (4) [26]:

$$P = P_0 \left(1 + D_p \times \frac{\Delta f}{f_N}\right) \quad (4)$$

Where P_0 is the pre-contingency active power consumption within the *study zone*, and Δf is the frequency deviation which can be expressed as below:

$$\Delta f = f - f_N \quad (5)$$

Where f_N is the nominal frequency. Furthermore, the load damping factor (D_p) can be calculated from (6).

$$D_p = \frac{\frac{\Delta P}{P_0}}{\frac{\Delta f}{f_N}} \quad (6)$$

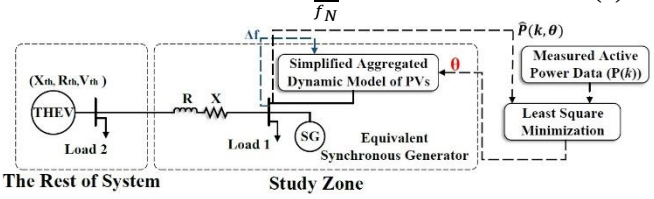

Fig. 4. The proposed closed-loop identification process and its associated simplified system model to reproduce the event under study

C. Coupling between Optimization Algorithm and Time-domain Simulation Tools

Once a new mutant vector $v_{i,g}$ is generated, a time-domain simulation is required to calculate the objective function in (1). It means that the time-domain simulation processing time has an impact on the identification processing time. It is thus advisable to use a software which requires less time to complete a time-domain simulation, while it is coupled to the optimization process so as to update the $\boldsymbol{\theta}$ vector to minimize the least-square error between the frequency response from the equivalent model and the actual frequency response. Once the unknown parameters are identified, the proposed dynamic equivalent model is ready to be integrated into a power system simulation tool to obtain the frequency response from utility-scale PV plants during the event under study.

IV. Case Studies

To evaluate the performance of the proposed dynamic equivalencing approach, the August 2018 separation event in Australia is considered in which contribution of utility-scale PV plants to frequency control was observed in Queensland (QLD) and South Australia (SA) [27]. The reader can refer to [17], [27-28] for more details on the August 2018 separation event in Australia.

A. Coupling between Optimization Algorithm and Time-domain Simulation Tool for the August 2018 Event Study

In this work, two simulation tools are used to simulate the frequency response provided by utility-scale PV plants during the event. Firstly, a software for phasor-mode time simulation, so-called RAMSES [29], is used as it features advanced model decomposition and parallelization techniques which strongly speed up a time-domain simulation. Then, the identification process is coupled with the RAMSES model so as to update the $\boldsymbol{\theta}$ vector to minimize the least-square error between the frequency response from the equivalent model and the actual frequency response reported in [17]. According to the Australian grid-code requirements, PV units must provide a 'one-shot' sustained droop response, responding and sustaining their output power to the maximum frequency deviation. In fact, once the frequency is recovering, PV units are not allowed to go back to their pre-event levels for 10 minutes [17]. Considering this requirement, an additional corrective term is then added to (1) to ensure that the unknown parameters are identified while the simulated maximum frequency deviation is close to the actual frequency overshoot. Therefore, the following objective function is used in this specific work:

$$\varepsilon_2(\boldsymbol{\theta}) = \varepsilon_1(\boldsymbol{\theta}) + \gamma|\Delta f_{smax} - \Delta f_{amax}| \quad (7)$$

Where Δf_{smax} is the simulated frequency overshoot and Δf_{amax} is the actual frequency overshoot observed during the event in a certain area. Once the parameters are identified, the equivalent model is integrated into the Australian 14-generator test system, implemented in MATLAB/SIMULINK [30], as a simplified version of the NEM transmission network, to reproduce the high-level frequency dynamic behavior witnessed in the August 2018 event.

B. Frequency Response from PV Units in Queensland

At the time of the event, 9 utility-scale PV farms were online with total output generation of 286.1 MW and total online capacity of 586 MW in QLD. According to the final report [17], 79 MW over-frequency droop response was provided by transmission-connected PV power plants in QLD following the Queensland-New South Wales Interconnector (QNI) trip due to multiple lightning strikes. Instead of modelling 9 utility-scale PV units, the proposed dynamic equivalent model is used to reduce the complexity of frequency stability analysis while improving the computational time. In fact, modelling 9 utility-scale PV plants will add at least 126 DAEs to the system model, while the dynamic equivalent model contains only 16 DAEs without consideration of technical delays. The simplified test-system model is constructed in RAMSES, using the data presented in Table I, to carry out the proposed closed-loop identification process. Table I also shows the parameters used in the optimization process. In this work, the DE algorithm terminates when $\varepsilon_2(\boldsymbol{\theta})$ decreases less than 0.1 during 10 successive iterations. To speed up the identification process, the measurement delay is aggregated to the coordination delay, thus $r_m = 0$ is assumed. Simulating the event for 35 seconds, the identification process is completed in 30 minutes after 55 iterations using a computer with an Intel(R) i7-6820 HQ quad-core processor @2.70 GHz, and 16 GB of RAM.

TABLE I. The Parameter Values of the Simplified Equivalent Model in RAMSES Used in the Identification Process

Parameter	Symbol	Value
QLD equivalent resistance	R	0.1 (Ω)
QLD equivalent reactance	X	1.089 (Ω)
QLD equivalent load	Load-1	5350 (MW)
Equivalent load of the rest of system	Load-2	1000 (MW)
Load damping factor	D_p	1
Thevenin equivalent resistance	R_{th}	4.16 (Ω)
Thevenin equivalent reactance	X_{th}	41.16 (Ω)
Thevenin short circuit MVA	S_{sc}	25000
Thevenin equivalent voltage	V_{th}	330 (kV)
Inertial constant of the equivalent SG	H	5 sec
Nominal MVA of the equivalent SG	S_{nom}	11000
Resistance of the equivalent SG	R_a	0
Reactance of the equivalent SG	X_l	0.15 (Ω)
Nominal voltage of the equivalent SG	V_t	330 (kV)
Weighted coefficient in (7)	γ	200

The parameters obtained via the proposed closed-loop identification process and presented in Table II. Since cascading failures and separation events are rare and the measurement data for such events is rare too, there is a difficulty in validation of the obtained parameters through other large disturbances. In this work, the robustness of the obtained parameters, at least, has been verified by running the DE algorithm for several times.

TABLE II. THE PARAMETER OF AGGREGATED DYNAMIC EQUIVALENT MODEL FOR UTILITY-SCALE PV UNITS IN QLD

Parameter	Value
F_{r-th}	50.4895 (Hz)
$F_{cut-off}$	51.04 (Hz)
PLL delay (δ_{PLL})	40 ms
r_m	0
r_c	1.1 sec

The dynamic equivalent model is then integrated into the 14-generator test system, as previously stated. Fig. 5 shows the simulated frequency response from dynamic equivalent model in QLD, the simulated QLD frequency, as well as the measured QLD frequency [17] following the QNI trip. First, the simulated QLD frequency is highly consistent with real measured frequency signal, reported in [17], in terms of overall frequency excursions, zenith point, and quasi steady-state frequency value. It also shows that the simulated frequency response (71 MW) is close to the actual frequency response provided by PV units in QLD (79 MW). Therefore, the proposed equivalent model is able to capture with good fidelity the aggregated frequency response from PV farms during the event. Further, over-frequency droop response from utility-scale PV units is generally different from typical over-frequency droop response from synchronous generators. This is because, as mentioned earlier, the aggregated PV output is required to be sustained also while the frequency is recovering, while synchronous generator provides a typical droop response.

It is also to be noted that although utility-scale PV units are in principle able to provide fast frequency response for the system thanks to fast converter response, the actual response was delivered ineffectively due to coordination delay. It is reported that the coordination delay was a result of built-in control system settings within the PV farms and it was unrelated to market outputs [17]. It is clear from Fig. 5 that the proposed method is also able to capture this technical delay as the simulated response is delivered to the system with 1.1 seconds delay.

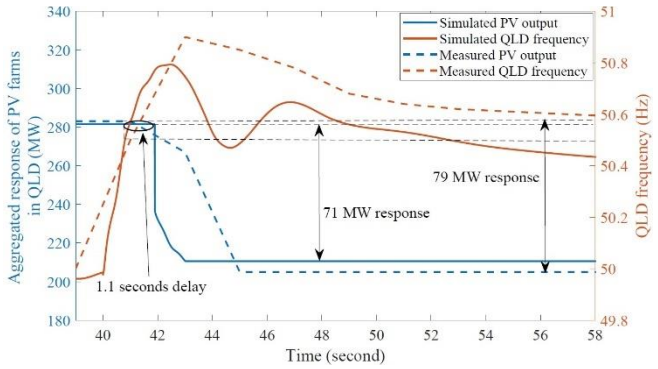

Fig. 5. The simulated frequency response from aggregated dynamic equivalent model in QLD as well as QLD's frequency

It is then interesting to try to understand how much response would have been provided from utility-scale PV plants if they had followed the grid-code requirements and there was no coordination delay. Based on our modelling and new simulations, Fig. 6 shows that utility-scale PV units could have delivered some 104 MW of aggregated frequency response if they had delivered a sustained droop response with no delay. So, the coordination delay has prevented PV farms to provide around 33 MW further frequency response in QLD. Finally, the QLD frequency could have been above 51 Hz if there was no frequency response from PV plants. This high frequency overshoot could result in generation disconnection in QLD. Indeed, the frequency control from PV plants in QLD contributed to the system resilience by reducing the likelihood of supply interruption.

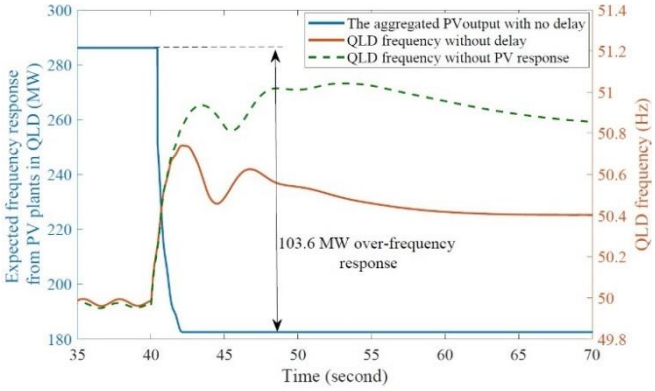

Fig. 6. The expected frequency response from aggregated PV plants in QLD as well as the QLD frequency without technical delays/PV response

C. Frequency Response from Utility-scale PV plants in South Australia

At the time of the event, there was only one utility-scale PV farm online in SA with output power of 89 MW and online capacity of 110 MW. It is reported that this PV plant was not able to control the frequency overshoot following the Heywood (interconnector between Victoria and SA) trip due to a huge delay around 4 seconds, from frequency measurement to plant reaction [17]. As before, the question arises as to how much frequency response could have been delivered in the SA system if the PV farm had responded faster. Considering the simulated SA frequency, Fig. 7 depicts how the utility-scale PV plant could have potentially delivered 83 MW over-frequency response. Also, it can be observed how once the frequency is recovering PV maintains its output power constant to comply with the grid-code requirements.

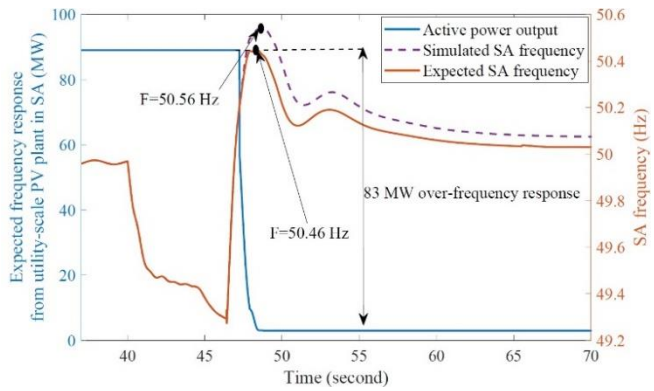

Fig. 7. The expected frequency response from the online utility-scale PV unit in SA as well as the SA frequency

V. CONCLUSION

This paper has presented a novel dynamic equivalent model for transmission-connected PV plants to reduce the

complexity of frequency stability analysis in PV-penetrated transmission networks. As the aggregated frequency response from several large-scale PV plants might differ from the frequency response provided by each individual PV farm, the dynamic equivalent model has been parametrized through a measurement-based identification process. A closed-loop identification process has then been proposed which employs a simplified system model to reproduce the frequency during the event under study, thereby taking into account the continuous impact of PV response on the system frequency, and eventually resulting in more accuracy in equivalent model parametrization. Also, the proposed dynamic equivalent model is developed to capture some possible technical issues which might negatively impact the frequency response performance of PV farms, such as coordination and measurement delays. Considering the August 2018 separation event in Australia, it has been shown how utility-scale PV units can participate in over-frequency control and system resilience. From the simulation results, it can be concluded that the proposed dynamic equivalencing approach is able to capture with good fidelity the aggregated frequency response from utility-scale PV units in QLD. Also, it has been discussed how measurement and coordination delays negatively affected the frequency response capabilities of transmission-connected PV units in SA and QLD, respectively. Finally, the model developed also allowed to assess the impact of these technical issues through a comparison between the responses that could have been expected response and the actual response.

As future work, even though the robustness of the proposed identification approach has been verified by multiple runs of the DE algorithm, we aim at validating the results we obtain in terms of uniqueness of the identified parameters through data from other large disturbances.

ACKNOWLEDGMENT

The authors would like to thank AusNet Services and Melbourne Energy Institute for their contribution and support to this work.

REFERENCES

[1] S. Eftekharnejad, V. Vittal, G. T. Heydt, B. Keel and J. Loehr, "Impact of increased penetration of photovoltaic generation on power systems," in *IEEE Trans. on Power Systems*, vol. 28, no. 2, pp. 893-901, 2013.

[2] S. Aupetit, M. Pokluda, "System protection behaviour and settings during system disturbances", Review Report for European Network of Transmission System Operators for Electricity, Tech. Rep. 2018.

[3] A. M. Stankovic and A. T. Saric, "Transient power system analysis with measurement-based gray box and hybrid dynamic equivalents," in *IEEE Trans. on Power Systems*, vol. 19, no. 1, pp. 455-462, 2004.

[4] Australian Energy Market Operator (AEMO), "Electricity rule change proposal, generator technical requirement", AEMO Information & Support Hub, Australia, 2017.

[5] National Renewable Energy Laboratory (NREL), "Demonstration of essential reliability services by a 300-MW solar photovoltaic power plant", Tech. Rep, 2017.

[6] Jun-Hee Hong and Jong-Keun Park, "A time-domain approach to transmission network equivalents via Prony analysis for electromagnetic transients analysis," in *IEEE Trans. on Power Systems*, vol. 10, no. 4, pp. 1789-1797, 1995.

[7] A. M. Stankovic and T. Aydin, "Analysis of asymmetrical faults in power systems using dynamic phasors," in *IEEE Trans. on Power Systems*, vol. 15, no. 3, pp. 1062-1068, 2000.

[8] G. C. Verghese, I. J. Perez-arriaga and F. C. Schweppe, "Selective Modal Analysis with Applications to Electric Power Systems, Part II: The Dynamic Stability Problem," in *IEEE Trans. on Power Apparatus and Systems*, vol. PAS-101, no. 9, pp. 3126-3134, 1982.

[9] R. Nath, S. S. Lamba and K. s. P. Rao, "Coherency Based System Decomposition into Study and External Areas Using Weak Coupling," in *IEEE Trans. on Power Apparatus and Systems*, vol. PAS-104, no. 6, pp. 1443-1449, 1985.

[10] IEEE Draft Guide for Synchronous Generator Modeling Practices and Parameter Verification with Applications in Power System Stability Analyses," in *IEEE P1110/D06*, 2018, vol., pp.1-91, 2019.

[11] Y. Liang, X. Lin, A. M. Gole and M. Yu, "Improved Coherency-Based Wide-Band Equivalents for Real-Time Digital Simulators," in *IEEE Trans. on Power Systems*, vol. 26, no. 3, pp. 1410-1417, 2011.

[12] S. Mat Zali and J. V. Milanović, "Generic Model of Active Distribution Network for Large Power System Stability Studies," in *IEEE Trans. on Power Systems*, vol. 28, no. 3, pp. 3126-3133, 2013.

[13] Z. Zhu, G. Geng and Q. Jiang, "Power System Dynamic Model Reduction Based on Extended Krylov Subspace Method," in *IEEE Trans. on Power Systems*, vol. 31, no. 6, pp. 4483-4494, 2016.

[14] A. M. Stankovic, A. T. Saric and M. Milosevic, "Identification of nonparametric dynamic power system equivalents with artificial neural networks," in *IEEE Trans. on Power Systems*, vol. 18, no. 4, pp. 1478-1486, 2003.

[15] G. Chaspierre, P. Panciatici and T. Van Cutsem, "Aggregated Dynamic Equivalent of a Distribution System Hosting Inverter-Based Generators," *2018 Power Systems Computation Conference (PSCC)*, Dublin, pp. 1-7, 2018.

[16] U. D. Annakkage *et al*., "Dynamic System Equivalents: A Survey of Available Techniques," in *IEEE Trans. on Power Delivery*, vol. 27, no. 1, pp. 411-420, Jan. 2012.

[17] Australian Energy Market Operator (AEMO), "Final report-Queensland and South Australia system separation on 25 August 2018", AEMO Information & Support Hub, Tech. Rep., 2019.

[18] S. I. Nanou, A. G. Papakonstantinou, S. A. Papathanassiou, "A generic model of two-stage grid-connected PV systems with primary frequency response and inertia emulation", *Electric Power Systems Research*, vol. 127, pp. 186-196, 2015.

[19] L. Chen, A. Amirahmadi, Q. Zhang, N. Kutkut and I. Batarseh, "Design and Implementation of Three-Phase Two-Stage Grid-Connected Module Integrated Converter," in *IEEE Trans. on Power Electronics*, vol. 29, no. 8, pp. 3881-3892, 2014.

[20] J. T. Bialasiewicz, "Renewable Energy Systems with Photovoltaic Power Generators: Operation and Modeling," in *IEEE Trans. on Industrial Electronics*, vol. 55, no. 7, pp. 2752-2758, 2008.

[21] J. S. Thorp, C. E. Seyler and A. G. Phadke, "Electromechanical wave propagation in large electric power systems," in *IEEE Trans. on Circuits and Systems I: Fundamental Theory and Applications*, vol. 45, no. 6, pp. 614-622, 1998.

[22] J. Nocedal and S. Wright, "Numerical optimization", *Springer Science & Business Media*, 2006.

[23] Conn, Andrew R., Katya Scheinberg, and Luis N, Vicente, "Introduction to derivative-free optimization", *SIAM Journal on Optimization*, vol. 8, 2009.

[24] K. Price, R. M. Storn, and J. A. Lampinen, "Differential Evolution – A Practical Approach to Global Optimization", Springer, 2005.

[25] G. Chaspierre, P. Panciatici, T.V. Cutsem, "Dynamic equivalent of a distribution grid hosting dispersed photovoltaic units", *IREP'17 Symposium*, Espinho, Portugal, 2017.

[26] P. Kundur, "Power system stability and control", *McGraw-Hill Inc*, New York, 1994.

[27] A. Jalali, M. G. Dozein and P. Mancarella, "Frequency Stability Provision from Battery Energy Storage System Considering Cascading Failures with Applications to Separation Events in Australia," *2019 IEEE Milan PowerTech*, Milan, Italy, pp. 1-6, 2019.

[28] M. Ghazavi Dozein, P. Mancarella, "Frequency response capabilities of utility-scale battery energy storgae systems, with application to the August 2018 separation event in Australia", *9th international conference on power and energy systems (ICPES2019)*, Perth, Australia, 2019.

[29] P. Aristidou, D. Fabozzi and T. Van Cutsem, "Dynamic Simulation of Large-Scale Power Systems Using a Parallel Schur-Complement-Based Decomposition Method," in *IEEE Trans. on Parallel and Distributed Systems*, vol. 25, no. 10, pp. 2561-2570, 2014.

[30] M. Gibbard and D. Vowles, "Simplified 14-generator model of the South East Australian power system," The University of Adelaide, pp. 1-138, 2014.